DEUTSCHES ELEKTRONEN-SYNCHROTRON
DESY 02-109
August 2002

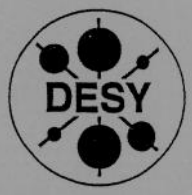

Temporal Propagators and Quasiparticles in Hot QCD

F. Karsch, E. Laermann, P. Petreczky, S. Stickan
Fakultät für Physik, Universität Bielefeld

I. Wetzorke
Deutsches Elektronen-Synchrotron DESY,
John von Neumann-Institut für Computing NIC, Zeuthen

ISSN 0418-9833

PLATANENALLEE 6 - 15738 ZEUTHEN

To be sure that your reports and preprints are promptly included in the HEP literature database
send them to (if possible by air mail):

DESY Zentralbibliothek Notkestraße 85 22603 Hamburg Germany	DESY Bibliothek Platanenallee 6 15738 Zeuthen Germany

DESY 02-109
August 2002

ISSN 0418-9833

Temporal propagators and quasiparticles in hot QCD

F. Karsch[1], E. Laermann[1], P. Petreczky[1], S. Stickan[1], and I. Wetzorke[2]

[1] Fakultät für Physik, Universität Bielefeld, Universitätsstraße 25, 33615 Bielefeld, Germany
[2] NIC/DESY Zeuthen, Platanenalle 6, D-15738 Zeuthen, Germany

1 Introduction

Strongly interacting matter undergoes a phase transition at some temperature T_c to a deconfined phase where it is believed that the dominant degrees of freedom are quasiparticles with quantum numbers of quarks and gluons contrary to the low temperature phase ($T < T_c$) where the dominant degrees of freedom are hadrons. The existence of this phase transition was shown using lattice Monte-Carlo simulations of Quantum Chromodynamics (QCD), the theory describing strongly interacting particles, some 20 years ago [1].

The deconfined high temperature phase of QCD is generally described as the plasma of strongly interacting matter. The dominant degrees of freedom are quarks and gluons, which a priori are massless degrees of freedom. At high temperature, however, they aquire a thermal mass resulting from interactions with the thermal heat bath. More precisely these masses represent a specific limit of the quark and gluon self-energies which have a rather complex energy (ω) and momentum ($\boldsymbol{p}$) dependence. At high temperature the quarks and gluons should thus be considered as quasi-particles propagating in the thermal heat-bath.

Quasiparticles show up as poles in the retarded quark and gluon propagators. The corresponding dispersion relations, the position of the poles, were studied in so-called HTL perturbation theory which is valid if the coupling constant $g(T)$ which controls the interaction among quarks and gluons becomes significantly smaller than unity and therefore a separation of different scales holds, $1/T \ll 1/gT \ll 1/g^2T$. These length scales characterize the typical scales over which thermal, electric and magnetic excitations propagate and thus also characterize the magnitude of corresponding quark and gluon masses (see e.g. [2] for a review). In the interesting temperature region close to the transition temperature T_c, however, the coupling is large $g \gtrsim 1$. Nevertheless, the corresponding quasiparticle picture finds application in refined perturbative calculations of the bulk thermodynamic properties where it helps to improve the convergence of the perturbative series [3] as well as in more phenomenological approaches [4]. In view of these facts a non-perturbative study of quark and gluon dispersion relations in the deconfined phase is highly desirable.

In the next section we describe in detail the goals of our project as well as some computational details. In section 3 we summarize our numerical results. Finally section 4 contains our conclusions.

2 Simulating finite temperature QCD on lattice

2.1 Goals and parameters of lattice Monte-Carlo simulation

Lattice Monte-Carlo simulations can provide information on the imaginary-time (Matsubara) propagator $D(i\omega_n, p)$ [2] (ω_n being the Matsubara frequencies). This is related to the retarded propagator by analytic continuation $D_R(p_0, p) = -D(p_0 + i\epsilon, p)$. This implies

$$D(i\omega_n, p) = -\int_{-\infty}^{+\infty} d\omega \frac{\rho(\omega, p)}{i\omega_n - \omega}, \tag{2.1}$$

where $\rho(\omega, p) = \frac{1}{\pi}\mathrm{Im}D_R(\omega + i\epsilon, p)$ is the spectral function. Quasiparticles (quarks and gluons) appear as complex poles in $D_R(p_0, p)$ or, equivalently, as peaks in the spectral function $\rho(\omega, p)$.

As quark and gluon propagators are gauge dependent quantities it is necessary to fix a particular gauge which we chose to be the Coulomb gauge. In this gauge the condition $\partial_i A_i(\tau, \boldsymbol{x}) = 0$ is imposed independently on different time slices which allows to construct a transfer matrix [5] [a] . As the consequence of this the spectral function of quarks and gluons is positive. Though the quark and gluon propagators are gauge dependent quantities the position of the peaks in the spectral function (poles in the retarded propagators) is gauge independent at any order of perturbation theory [6]. Gauge independence of the peak position can be proven also non-perturbatively in a class of gauges which allow the construction of a transfer matrix [5]. At finite temperature there are two kinds of quasiparticle excitations (corresponding to two branches in the dispersion relation) [2]: (i) the real quasiparticles (quarks and transverse gluons), which are the analog of partonic degrees of freedom at zero temperature, and (ii) collective excitations (plasmino and longitudinal gluons), which have exponentially small residues for momenta $p > T$.

We calculated the temporal quark and gluon propagators, i.e. the propagators in the mixed (τ, p)-representation (τ being the imaginary time),

$$D(\tau, p) = \sum_n D(i\omega_n, p) \exp(-i\omega_n \tau) \tag{2.2}$$

[a] To fix the gauge completely an additional time-dependent gauge transformation is necessary. This, however, depends on temporal link variables $U_0(\tau, x) \equiv \exp(iagA_0(\tau, x))$ only [8].

for several values of the spatial momenta p. Using Eq. (2.1) the gluon propagator in the mixed representation can immediately be written in terms of the spectral function,

$$D^g_{(T,L)}(\tau,p) = \int_0^\infty d\omega \rho_{(T,L)}(\omega,p) \frac{\cosh(\omega(\tau - 1/2T))}{\sinh(\omega/2T)}, \tag{2.3}$$

where T and L refer to transverse and longitudinal gluons respectively. The most general form of the temporal quark propagator is

$$D^q(\tau,p) = \gamma_0 F(\tau,p) + \boldsymbol{\gamma}\cdot\boldsymbol{n} G(\tau,p) + H(\tau,p), \tag{2.4}$$

with $\boldsymbol{n} = \boldsymbol{p}/p$. In the chiral limit the last term vanishes. Using the most general form for the retarded quark propagator [7] and Eq.(2.1) one can derive the following representation for the functions F and G:

$$F(\tau,p) = \int_0^\infty d\omega \rho_F(\omega,p) \frac{\cosh\omega(\tau - 1/2T))}{\cosh(\omega/2T)}\ , \tag{2.5}$$

$$G(\tau,p) = \int_0^\infty d\omega \rho_G(\omega,p) \frac{\sinh\omega(\tau - 1/2T))}{\cosh(\omega/2T)}\ . \tag{2.6}$$

Equations (2.3), (2.5) and (2.6) relate the temporal propagators which we calculate to the spectral function and thus in principle can be used to reconstruct the spectral functions. However, the propagators are calculated for ~ 10 values of τ while for any reasonable discretization of the ω-range the spectral function $\rho(\omega)$ is parameterized by ~ 100 parameters. This clearly is an ill-posed problem and additional input is needed to fix these parameters. In order to do so we use the *Maximum Entropy Method* (MEM) (see [9] for a review). In this approach one searches for a spectral function which maximizes the quantity $\alpha S - L$, where L is the likelihood function corresponding to the standard χ^2-fit, α is a real parameter and S is an entropy functional which incorporates any prior knowledge on the structure of the spectral function through the so-called default model $m(\omega)$ [9]. For a positive definite spectral function $\rho(\omega)$, $S[\rho(\omega), m(\omega)]$ is the Shannon-Jaynes entropy (for other cases see [10])

$$S[\rho(\omega), m(\omega)] = \int_0^\infty d\omega(\rho(\omega) - m(\omega) - \rho(\omega)\ln\frac{\rho(\omega}{m(\omega)})). \tag{2.7}$$

Now we need to specify the default model. From Eqs. (2.3), (2.5) and (2.6) one can see that $\rho_{T,L}$ and $\rho_{F,G}$ have dimension of inverse mass squared and inverse mass respectively. For large ω the spectral functions can be calculated using perturbation theory. On the other hand if ω is large enough it is the only dimensionful scale. Therefore

$$\rho_T(\omega\to\infty) = m_0^T/\omega^2, \tag{2.8}$$

$$\rho_F(\omega\to\infty) = \rho_G(\omega\to\infty) = m_0^F/\omega, \tag{2.9}$$

where $m_0^{T,F}$ is a dimensionless real number and $m_0 \sim \mathcal{O}(\alpha_s)$ (in what follows we omit the superscript on m_0).

2.2 Simulation Programme and CPU requirements.

We have performed simulations in quenched QCD[b] with Wilson fermions on isotropic (i.e. with the same lattice spacing in time and space like directions) $64^3 \times 16$ lattices. Propagators have been calculated at two values of the temperature, $1.5T_c$ (corresponding to gauge coupling $\beta = 6.972$) using 20 gauge configurations and at $3T_c$ ($\beta = 7.457$) using 40 gauge configurations.

Because of the large memory requirements of our calculations we have separated the various steps into three independent programs: generation of gauge configurations, gauge fixing and calculations of the propagators. The typical memory requirement at each of these steps is about 500Mwords (4GByte).

The programs for gauge field updates, gauge fixing and calculation of the propagators have been written in FORTRAN 90 and use MPI. In the generation of gauge field configurations we use the Kennedy-Pendleton heatbath algorithm [12] combined with an overrelaxation step to simulate the SU(3) gauge theory. In fact, here we use 4 overrelaxation steps followed by one heatbath update. The acceptance rate of the update routine is about 98%. We have performed simulations on 4-dimensional lattices of size $64^3 \times 16$. To perform simulation on such large lattices at least 64 PEs have to be used in order to satisfy the overall memory requirements (assuming 128 MB per node). For one complete update of gauge fields on the T3E-900 (1 heatbath and 4 overrelaxation steps) we need 44.74 sec on 64 PEs. We have performed simulations at two temperatures, $3T_c$ and $1.5T_c$. For these we found that the typical autocorrelation time characterizing the decorrelation of subsequent gauge field configurations is about 100 (200). Thus we need 100 (200) updates to produce one independent configuration. This means that in order to generate one independent configuration for the two temperatures considered we needed 238.6 CPUh (normalized to the time per processor unit).

In our analysis of propagators we use the Coulomb gauge. The gauge fixing routines for Coulomb gauge use the overrelaxation algorithm [13]. We find that this

[b] for a recent review, further references and introductory articles see [11].

gauge fixing algorithm is very efficient. The typical number of iterations required to fix the Coulomb gauge on a configuration with accuracy $|\partial_i A_i|^2 < 10^{-6}$ is about 1300. As an alternative we have tested an algorithm based on Fast Fourier Transformation which needs approximately 300 iterations to achieve the same accuracy on a $32^3 \times 4$ lattice. It, however, is 5-6 times more expensive in terms of CPU time. Still, the gauge fixing is the most time consuming part of the project. The costs of gauge fixing of one configuration is 305.3 CPUh.

3 Numerical results

In this section we will summarize our numerical results on the temporal quark and gluon propagators and on the quasiparticle properties extracted from them. Some preliminary results have been published in [14,15].

3.1 Temporal quark and gluon propagators

First let us summarize our numerical results for the temporal propagators. The finite lattice volume introduces an infrared cutoff, the smallest non-zero momentum available on our $(64^3 \times 16)$ lattice is $p_{min} = 1.57T$ which is quite large. Because of this we cannot resolve the particular behavior of the collective excitations. In particular the longitudinal gluon propagator is compatible with zero within present statistical accuracy. The temporal gluon propagators are influenced by a zero Matsubara mode contribution $D^g_{(T,L)}(i\omega_n = 0, p)$, which is the static magnetic propagator in momentum space studied in detail in Ref. [8]. At $p = 0$ the magnetic propagators are strongly volume dependent and very large lattices are needed to perform a reliable infinite volume extrapolation [8]. As a consequence the dispersion relation at zero momentum , i.e the plasmon frequency ω_P, cannot be reliably determined from our present calculations. Therefore in what follows the gluon propagators are analyzed only for non-zero momenta.

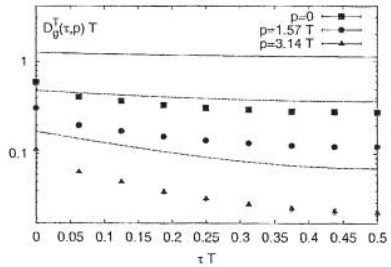

Fig. 1. The transverse gluon propagator for different momenta. The solid, dashed and dashed-dotted lines correspond to the prediction of perturbation theory in HTL approximation for momenta $p/T = 0,\ 1.57$ and 3.14 respectively.

For high temperatures (considerably larger than T_c) one expects that perturbative calculations based on Hard Thermal Loop (HTL) approximation should work [2]. Therefore we compare our data for temporal quark and gluon propagators with the predictions of perturbation theory in HTL approximation at $T = 3T_c$. In Figure 1 we show our results for the transverse gluon propagator $D^T_g(\tau, p)$ at three values of the spatial momenta calculated on 40 gauge fixed configurations. We also show there the prediction of the HTL approximation using a coupling constant $g \simeq 1.6$ suggested by the short distance behavior of the heavy-quark potential [14]. As one can see from the figure the data deviate substantially from the HTL prediction even at momenta $p = 3.14T$. We note that corrections to the HTL approximation will not resolve this discrepancy since they lead to smaller $\omega(p)$ values shifting the propagator to values larger than the HTL result [16].

Let us now discuss the quark propagators. First we note that $H(\tau, p)$ is zero within present statistical accuracy for both temperatures and all values of the spatial momenta considered. In Figure 2 we show our results for $F(\tau, p)$ calculated on 40 configurations and compared with predictions of the HTL approximation. As in the case of the gluon propagator we find large deviations from the HTL predictions. The situation is similar for $G(\tau, p)$. We have found that there is no choice of g which can provide agreement between lattice results and HTL.

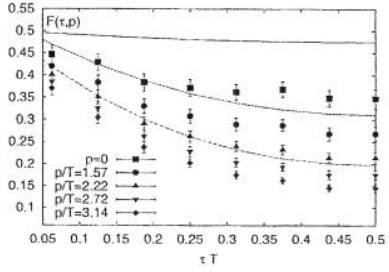

Fig. 2. The quark propagators for different momenta. The solid, dashed and dashed-dotted lines correspond to the prediction of perturbation theory in HTL approximation for momenta $p/T = 0,\ 1.57$ and 3.14 respectively.

3.2 Determination of the spectral functions

As discussed already in section 2.1, the spectral functions are reconstructed from temporal quark and gluon correlators. First of all we are interested in the position of peaks in the spectral functions as these determine the dispersion relations of quasiparticles and as such are expected to be gauge-independent. At zero temperature the peaks in the spectral function can also be determined from exponential fits to the large distance behavior of the different correlators. Alternatively one can determine

them from so-called effective masses, which reach a plateau at large distances. At finite temperature both methods are inadequate for the determination of the peak position as the temporal lattice extent is always limited by the inverse temperature. However, if the spectral function is dominated by a single particle state than effective masses may still be used to determine the dispersion relation. The effective masses are introduced by the following formula for $D_T(\tau,p)$ and $F(\tau,p)$

$$\frac{D(\tau,p)}{D(\tau+1,p)} = \frac{\cosh(m(\tau)(\tau-1/(2T)))}{\cosh(m(\tau)(\tau+1-1/(2T)))}, \tag{3.1}$$

with D being $D_T(\tau,p)$, $F(\tau,p)$, while for $G(\tau,p)$ it is defined as

$$\frac{G(\tau,p)}{G(\tau+1,p)} = \frac{\sinh(m(\tau)(\tau-1/(2T)))}{\sinh(m(\tau)(\tau+1-1/(2T)))}. \tag{3.2}$$

First let us discuss the gluon spectral function. In Figure 3 we show the gluon spectral function at $T = 3T_c$ and for $p = 1.57T$. One can see a rather broad peak around $\omega/T \sim 2$ and a very broad structure for $\omega > 10T$. The spectral function itself strongly depends on the default model parameterized by m_0. The position of the peak, however, is not influenced by the default model at least within the present statistical accuracy. At finite temperature the gluonic quasiparticle peak can also aquire a finite width due to thermal effects [2]. However, the width observed by us at present seems to be primarily due to insufficient statistics and too few data points used in the analysis. A similar conclusion has been drawn in [9]. In Figure 3 we also show the effective masses from the temporal gluon propagator for $T = 3T_c$ and $p = 1.57T$, where the peak position from the MEM analysis is also shown. As one can see from the Figure the effective masses do not reach a plateau and stay above the peak position extracted from the MEM analysis. This is in accordance with the observation that the spectral function receives large contributions from $\omega \gg p$. The situation is similar for other values of the spatial momenta and temperature.

Now we turn to the discussion of the quark propagators. It turns out that our data on G are too noisy to apply the MEM analysis to them. The local masses extracted from F and G, however, are identical within statistical errors. In fact, if the quark propagators are dominated by a single quasiparticle contribution, the local masses extracted from F and G should be identical. We therefore applied the MEM analysis only for F. The reconstructed spectral function $\rho_F(\omega,p)$ is shown in Figure 4. It has only a single peak indicating the absence of the plasmino branch for the values of the momenta studied by us (at zero momentum there is no distinction between the quasiparticle (quark) and plasmino branch). In contrast to the gluon spectral function the quark spectral function extracted from F has negligible continuum contribution above the light cone. As a consequence the corresponding effective masses $m_q(\tau,p)$ shown in Figure 4 reach a plateau already at $\tau T = 0.065$. The

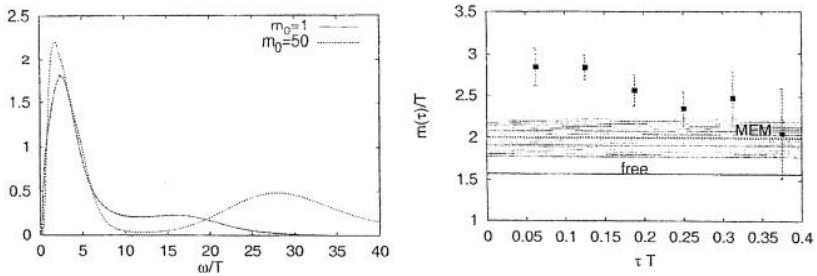

Fig. 3. The gluon spectral function for $3T_c$ and $p = 1.57T$ (left) and effective gluon mass (right). The dashed line and the band on the right figure is the position of the peak of the spectral function from the MEM analysis and its uncertainty.

position of the peak in the spectral function $\omega_q(p)$ agrees with the average value of the local masses $m_q(\tau,p)$.

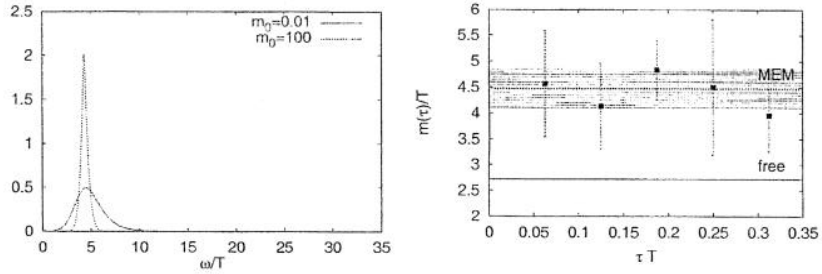

Fig. 4. The quark spectral function for $T = 1.5T_c$ and $p = 2.72T$ (left) and the corresponding local masses (right). The dashed line and the band on the right figure are the peak position from the MEM analysis and uncertainty of its value.

3.3 Dispersion relation and quasiparticle masses

Performing the analysis described in the previous section for all values of the spatial momenta we can determine the dispersion relations of quarks and gluons, $\omega_q(p)$ and $\omega_g(p)$.

Our numerical results for the dispersion relations of quark and gluons $\omega_q(p)$ and $\omega_g(p)$ are summarized in Figure 5. While at $T = 3T_c$ the dispersion relation both for quarks and gluons is close to the free dispersion relation $\omega^2(p) = p^2$ one sees large deviations from it at $T = 1.5T_c$. In order to quantify the deviations from the

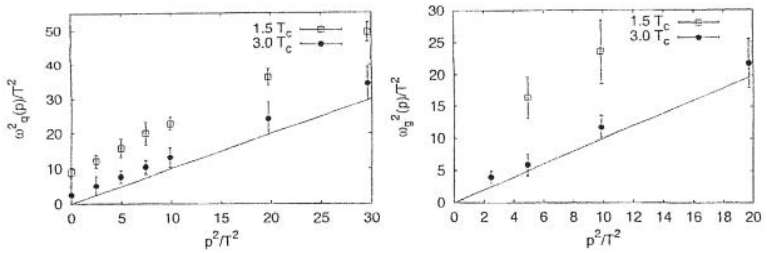

Fig. 5. The dispersion relation of quarks (left) and gluons (right) for temperatures $T = 1.5T_c$ and $3T_c$.

free propagation we have fitted the dispersion relations to $\omega^2_{q,g}(p) = p^2 + m^2_{q,g}$ and determined the values of quasiparticle masses m_q and m_g. For $T = 3T_c$ we have found $m_q/T = 1.7 \pm 0.1$ and $m_g/T = 1.2 \pm 0.1$. The value of the gluon mass is compatible with the leading order result of HTL perturbation theory $m_g^2 = g^2T^2/2$ if we assume for the gauge coupling $g(3T_c) \sim 1.6$ as suggested by the short distance behavior of the heavy quark potential [14]. With the same value of g the leading HTL result for m_q is roughly a factor 2 smaller than the value found by us. For $T = 1.5T_c$ we have obtained $m_q/T = 3.9 \pm 0.2$, $m_g/T = 3.4 \pm 0.3$. Here the value of m_q was obtained by omitting the first three values of $\omega_q(p)$ from the fit. The values of the quasiparticle masses at $T = 1.5T_c$ are considerably larger than the corresponding ones at $3T_c$ and those expected from perturbation theory. This is consistent with the temperature dependence of quasiparticle masses $m_{q,g}/T$ used in quasiparticle models for the equation of state [4].

4 Conclusions

We have calculated the temporal quark and gluon propagators on large ($64^3 \times 16$) isotropic lattice and extracted the spectral function from them. Calculating the spectral function at several spatial momenta we were able to determine the dispersion relation for quarks and gluons and extract the temperature dependent quasiparticle masses. We have found that the quasiparticle masses measured in units of temperature increase substantially as the temperature is lowered from $3T_c$ to $1.5T_c$.

Our temporal propagators are quite different from those calculated within the HTL perturbation theory. We have found that in general medium effects are stronger than suggested by hard thermal loop perturbation theory. In particular, the quasiparticle masses determined by us are generally larger than those predicted by HTL perturbation theory (except for the gluon mass at $3T_c$). We also see a large continuum contribution in the gluon spectral function which is absent in the HTL approximation.

Due to the finite lattice volume we were not able to resolve collective mode such as the plasmino mode. For a detailed study of these modes one should consider even larger spatial volumes which eventually will become possible by considering anisotropic lattices with spatial lattice spacing larger than the temporal one.

References

1. J. Kuti et al, Phys. Lett. **B98** (1981) 199; L.D. McLerran and B. Svetitsky, Phys. Rev. **D24** (1981) 450; J. Engels, F. Karsch, H. Satz and I. Montvay, Phys. Lett. **B101** (1981) 89
2. M. Le Bellac, *Thermal Field Theory* (Cambridge University Press 1996)
3. F. Karsch et al, Phys. Lett. **B401** (1997) 69; O.J. Andersen et al, Phys. Rev. Lett. **83** (1999) 2139; J.P. Blaizot et al, Phys. Rev. Lett. **83** (1999) 2906
4. U. Heinz and P. Levai, Phys. Rev. **C57** (1998) 1879; A. Peshier et al, Phys.Rev. **C61** (2000) 045203
5. O. Philipsen, Phys. Lett. **B521** (2001) 273; hep-lat/0112047
6. R. Kobes et al. Nucl. Phys. **B355** (1991) 1; A.S. Kronfeld, Phys. Rev. **D58** (1998) 051501
7. A. Weldon, Phys. Rev. **D61** (2000) 036003
8. A. Cucchieri et al, Phys. Lett. **B497** (2001) 80; Phys. Rev. **D64** (2001) 036001
9. M. Asakawa et al, Prog. Part. Nucl. Phys. **46** (2001) 459
10. K. Langfeld et al, Nucl. Phys. **B621** (2002) 131
11. F. Karsch, Lect. Notes Phys. **583** (2002) 209 (hep-lat/0106019)
12. A.D. Kennedy and B.J. Pendleton, Phys. Lett. **B156** (1985) 393
13. F. Karsch and J. Rank, Nucl. Phys. B (Proc. Suppl.) **42** (1995) 508
14. P. Petreczky et al, Nucl. Phys. **A698** (2002) 400
15. P. Petreczky et al, Nucl. Phys. B (Proc. Suppl.) **106** (2002) 514
16. H. Schulz, Nucl. Phys. **B413** (1994) 353; A. Peshier et al, Ann. Phys. **266** (1998) 162